ELSEVIER

Journal of Power Sources 97–98 (2001) 826–831

JOURNAL OF POWER SOURCES

www.elsevier.com/locate/jpowsour

Challenges in making of thin films for $Li_xMn_yO_4$ rechargeable lithium batteries for MEMS

D. Singh[a,*], R. Houriet[a], R. Giovannini[a], H. Hofmann[a], V. Craciun[b,1], R.K. Singh[b]

[a]*Powder Technology Laboratory (LTP), Department of Materials Science, Swiss Federal Institute of Technology (EPFL), CH 1015 Lausanne, Switzerland*

[b]*Department of Materials Science and Engineering, University of Florida, Gainesville, FL 32611, USA*

Received 20 June 2000; accepted 13 January 2001

Abstract

Microelectromechanical systems also known as MEMS are used in various small-scale sensor applications. A new trend is witnessed in the MEMS industry called ''system on a chip''. The goal is to develop a chip with a sensor, an actuator and power source and power storage device all on one chip. $LiMn_2O_4$ thin films show great promise as providers of power to these sensors and actuators on a silicon chip. These batteries are required to have high power density, high charge and discharge rate capability, long cycle life and reduced capacity fading. To demonstrate these features pulsed laser deposition (PLD) and the laser spark atomization (LSA) techniques were used to deposit $LiMn_2O_4$ films on various substrate materials. The thin (<0.2 μm) films grown by PLD were highly crystalline and textured along either (1 1 1) or (0 0 1) direction depending on the substrate type. Films grown by LSA were much thicker (>1 μm) and exhibited a porous structure consisting of a mixture of randomly oriented nanocrystals embedded in an amorphous matrix. The effect of these two different microstructures on the electrochemical properties of the $LiMn_2O_4$ thin films has been investigated. The results obtained indicate that differences in film structure and particle morphology have a significant impact upon electrochemical kinetics of Li ion intercalation and de-intercalation.

Keywords: Microelectromechanical systems; Sensors; Actuators

1. Introduction

Microelectromechanical systems(MEMS) are used as small scale sensors for a wide variety of applications. A MEMS device consists of a sensor, an actuator, power conversion and storage device. A new trend is now being witnessed in the MEMS industry in which all the above parts are being placed on a single chip and this is called a ''system on a chip''. Power providers required for the operation of these sensors and actuators must meet certain requirements. The component size of the power device should be compatible with the MEMS structure. It should be integrated onto a silicon chip under standard processing conditions. It should have no moving parts and have a solid state construction. It should be efficient with minimal thermal loss. The power storage component should have high power density, high rate capability with a long cycle life [1,2,11].

$LiMn_2O_4$ thin films show great promise as power providers for these applications. In this study $LiMn_2O_4$ thin film batteries were investigated to see if they exhibit long cycle life, reduced capacity fading high power density and high charge and discharge capability. To investigate the different properties of $LiMn_2O_4$ structure two laser deposition techniques were used. Films were deposited on various substrates using the laser spark atomizer (LSA) and the pulsed laser deposition (PLD). LSA method gives porous films, whereas the PLD technique allows the formation of crystalline and dense films. These films were characterized by XRD, RBS, scanning electron microscope and electrochemical measurements. Kinetics of these films were determined by cyclic voltammetery and galvanostatic tests. The relation between film microstructure and electrochemical performance has been better understood by means of these characterizations.

$LiMn_2O_4$ thin films have been synthesized by various deposition techniques such as chemical vapor deposition [3], rf sputtering [4] and PLD [5,6]. All these techniques are followed by a high temperature anneal which causes Li deficiency in the film [16]. Deposition at low temperatures

* Corresponding author.
E-mail address: deepikasingh@hotmail.com (D. Singh).
[1] Present address: Institute of Atomic Physics, Bucharest, Romania.

0378-7753/01/$ – see front matter
PII: S0378-7753(01)00704-2

by magnetron sputtering shows poor crystallinity and nanocrystalline morphology. The electrochemical performance is better suited for low power applications. Thus, we have investigated two laser deposition techniques which are conducted at high and low temperatures. The PLD technique is particularly suited for the growth of multicomponent thin films [7,8] because of the stoichiometric transfer of material from target to the growing film. Since it is well known that the microstructure of the $LiMn_2O_4$ thin film intimately controls its electrochemical characteristic [9], we decided to investigate this relation in more detail. In this study, we have explored the use of the laser-based techniques such as PLD and LSA to change the microstructure of the grown films from randomly oriented nanocrystalline phase to highly oriented polycrystalline film and correlate it with the film electrochemical properties.

2. Experimental

Pulsed laser deposition was used to deposit thin films of $LiMn_2O_4$ on stainless steel and monocrystalline (1 0 0) Si substrates. A pulsed excimer laser ($\lambda = 248$ nm, pulsed duration 25 ns) impinges on the $LiMn_2O_4$ target, which is continuously rotated to avoid the formation of a deep hole. The target was formed from commercial $LiMn_2O_4$ powder, which was cold pressed and sintered at 800°C for 12 h. As the stoichiometry during laser deposition is maintained, the best results are typically obtained using single phase targets. Due to the expansion hydrodynamics of the ablated material, the laser plume expands normal to the target material and is collected onto the substrate [7]. All films were deposited with a fluence of approximately 1 J/cm^2 and either 3000 or 6000 laser pulses. The chamber was pumped down to a base pressure of at least 10^{-6} Torr and then backfilled with oxygen at a pressure of 200 mTorr. The substrate was placed on a resistive heater located parallel at a distance of approximately 5 cm away from the target. The deposition temperature was set in the 650–750°C range.

A modification of the conventional laser ablation technique, the LSA process was the other method used to deposit thick coatings (∼1 μm). The major difference between these two techniques is the nature of the gas-phase precursor species that are collected on the substrate. In the PLD process, the depositing species are typically atomic in nature, whereas because of the high pressure (∼1 atm) employed in the LSA method, the expansion plume is confined and the atoms condense creating nanometer-sized clusters, which are afterwards deposited onto the substrate. Due to the relatively large size of the deposition species and low substrate temperature, the films deposited by this technique are not dense, but form a tri-dimensional mesoporous network of nanoparticles assembled in a web-like structure [10]. These films were deposited on stainless steel grids and afterwards annealed in air at 600–700°C.

The grown films were characterized using X-ray diffraction (XRD) and scanning electron microscopy (SEM). For electrochemical characterization, half-cells consisting of the $LiMn_2O_4$ film as the cathode and Li metal as the anode and reference electrode were used. 1 M $LiClO_4$ in propylene carbonate (PC) was employed as electrolyte in the half-cells. The ac impedance, cyclic voltammetery, and galvanostatic cycling measurements of the formed cells were conducted.

3. Results

3.1. Microstructural characterization

The films grown using PLD were highly crystalline and exhibited textured growth. The texturing was mainly dependent on the deposition temperature and the nature of the substrate. Fig. 1 shows the XRD pattern of the films deposited on doped silicon. The films deposited on silicon at

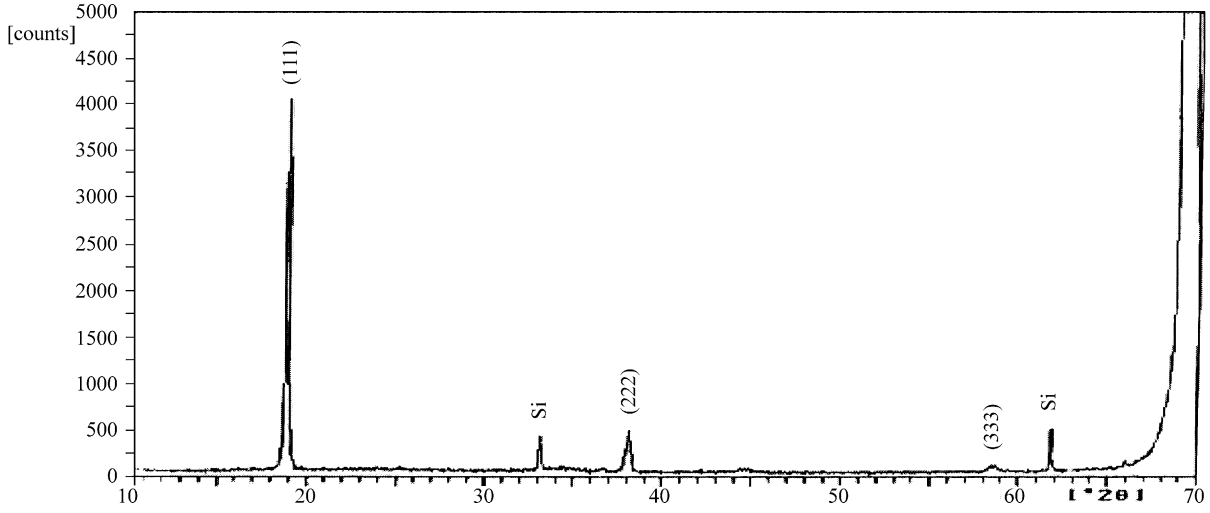

Fig. 1. XRD pattern of a thin film deposited on conductive silicon substrate using PLD.

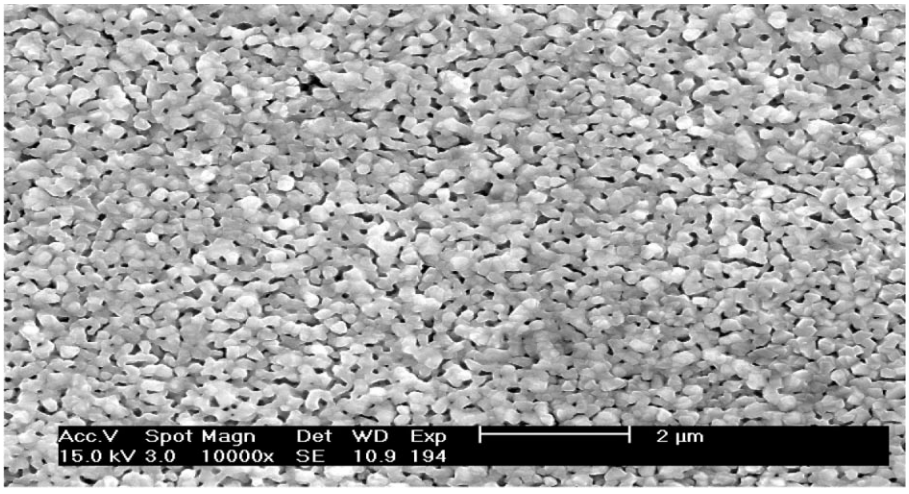

Fig. 2. Typical SEM micrograph of a $LiMn_2O_4$ thin film using PLD.

temperatures above 650°C exhibited only the (1 1 1) orientation while those deposited on stainless steel exhibited a (0 0 1) orientation. A mixed orientation, was found when the films were deposited on stainless steel grid, most likely because of the lower deposition temperature due to the poor thermal contact between the grid and heater. The XRD peaks are quite sharp, suggesting the presence of large crystalline grains in the film. This was confirmed by SEM investigations of the morphology of the films grown on stainless steel substrates, which showed well formed grains with an approximate size of 200 nm, as one can see in Fig. 2. The grains were equiaxed in two dimensions and densely packed in the film. Films deposited on other substrates such as sapphire, nickel substrates under identical conditions exhibited poorer crystallinity and their electrochemical properties were not investigated. Despite the good crystallinity there are certain disadvantageous of using high substrate temperatures. Li deficiency is observed at higher substrate temperature. Use of higher oxygen pressure can slightly overcome this effect [5]. At higher deposition temperatures, cross contamination due to diffusion across the substrate may occur. High temperatures are also not compatible with silicon processing.

By contrast, the films deposited by the LSA method possessed a completely different microstructure. The XRD pattern of a film deposited using LSA is displayed in Fig. 3, while its structure morphology is shown in Fig. 4. The XRD pattern shows a broad background peak with a few rather weak intensity crystalline diffraction peaks. Based on the width of the weak X-ray diffraction peaks, one can assume that this signal arises from small nanometer-sized crystalline regions in the film matrix. The broad background peak seen between ∼15 and 30° corresponds to a predominant amorphous phase. SEM micrographs of the morphology of the film like those displayed in Fig. 5 showed that the film is composed of fractal-like aggregates of nanoparticles. From such micrographs, the overall porosity of the film was estimated to be around 90%. The surface area of this film was measured to be 17 m^2/gm. The film had poor adherence to the substrate and, thus, was very fragile.

3.2. Electrochemical measurements

The PLD films grown on stainless steel were subjected to extended cycling at a charge and discharge rate of 100 μA (approximately 15–20°C) between a voltage range of 3.5 and 4.4 V versus Li/Li^+ electrode. All electrochemical measurements were performed in argon filled glove box at room temperature. A slight polarization was observed towards the end of charge due to the use of very high charge rates. Despite the high rates of charge and discharge, a good cyclability of the films was observed, the discharge capacity after 200 cycles being 93% of the 100th cycle capacity as one can see in Fig. 5. Similar stability in discharge capacity was reported for thin films prepared by the PLD and rf sputtering process [12]. The good cyclability of the thin films in comparison to the capacity fading phenomenon usually observed for powders may be attributed to the highly ordered structure of $LiMn_2O_4$ in the thin film electrode,

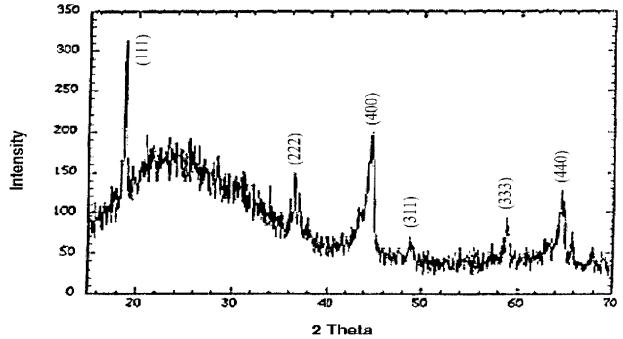

Fig. 3. XRD pattern of a $LiMn_2O_4$ film deposited on a stainless steel grid substrate using LSA.

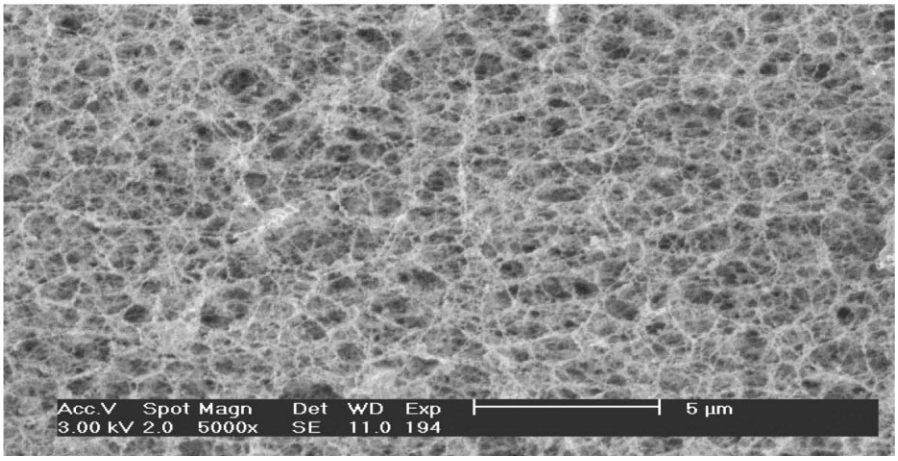

Fig. 4. SEM micrograph of a $LiMn_2O_4$ thick film deposited on a stainless steel grid substrate using LSA.

absence of carbon in the structure and lower inherent stresses in thin film electrodes [12].

The effect of various discharge rates ranging from 100 to 500 μA was also studied and is shown in Fig. 5. A large capacity loss and a decrease in operating discharge voltage were observed when the discharge rate was increased from 100 to 500 μA. When very high charge and discharge rates were used, the charge and discharge efficiency of the cell was significantly affected. The slow decrease in operating voltage at high rates can be attributed to the diffusion polarization caused by Li intercalation and de-intercalation kinetics. As a result of diffusion polarization, an increased over potential is reached at a faster rate when higher charge currents are used, thus, preventing the cells from charging efficiently. Diffusion of lithium ions also limits discharging efficiency at higher discharge rates. Therefore, a larger capacity loss along with lower operating discharge voltage is observed when higher charge and discharge rates are used [13,14].

Fig. 6 displays the cyclic voltammogram of a $LiMn_2O_4$ thin film deposited on a stainless steel grid using the PLD technique. The average thickness of the film was ∼0.1 μm. The film was cycled between 3.5 and 4.5 V at a scan rate of 0.1 mV/s. The two peaks on charge were located at 4.05 and 4.19 V, while on discharge they were located at 3.9 and 4.11 V. These peaks correspond to the two-step reversible de-intercalation and intercalation of lithium in $LiMn_2O_4$ [15]. The acquired voltammogram, which is shown in Fig. 8, represents a reversible diffusion controlled process with good repeatability. The cyclic voltammogram of a typical LSA film is shown in Fig. 7. The voltammogram obtained from this film exhibits high degree of capacitance. This can be correlated with the nanocrystalline nature of the film and a high surface area. The redox peaks obtained from these films were sharp and exhibit low currents. However, the film showed good reversibility and repeatability.

The effect of scan rates was also studied. As discussed in previous sections, the XRD results indicated a very highly

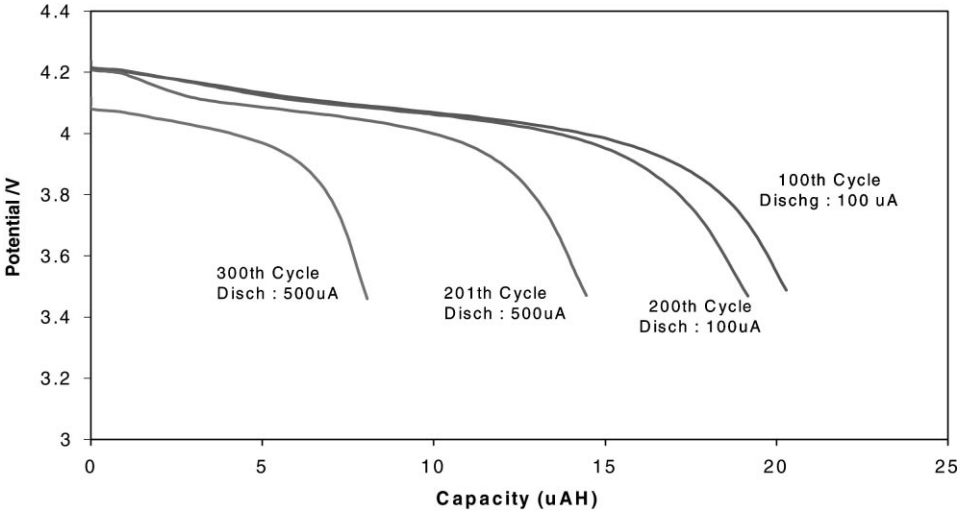

Fig. 5. Discharge capacity comparison between different cycles at various discharge rate.

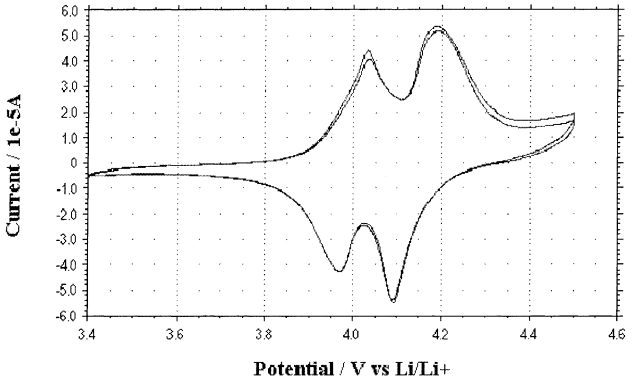

Fig. 6. Cyclic voltammogram of a 0.1 μm thick PLD $LiMn_2O_4$ film cycled between 3.5 and 4.5 V vs. Li/Li^+ with 1 M $LiClO_4$ in PC electrolyte at a scan rate of 0.1 mV/s.

crystalline structure for the thin films deposited by PLD, while a mixed phase of nanocrystals within an amorphous phase was indicated for the LSA deposited film. The cyclic voltammograms recorded at various scan rates for a PLD film are displayed in Fig. 8and those of a LSA film are displayed in Fig. 9. A comparison between Figs. 8 and 9 shows that the shape of the curve is strongly affected by the morphology of the films.

An increase in scan rate (v) decreases the apparent number of electroactive species (and the current) involved in the overall process. It also causes current density as a function of scan rate, denoted here by I/v, to decrease and, thus, the peak height is considerably reduced [14]. At higher scan rates a progressive shift of the peaks to a higher potential value is observed during charge while a shift to a lower potential is observed during discharge. Fig. 9 exhibits well-resolved peaks for all various scan rates used while Fig. 8 only exhibits poorly resolved peaks. The change in peak shape with scan rate can be correlated to the kinetics of lithium intercalation and de-intercalation at the electrode/electrolyte interface and the rate of lithium diffusion in the film. A wave-like shape instead of a sharp peak is observed when the reaction kinetics including the diffusion of lithium are slow

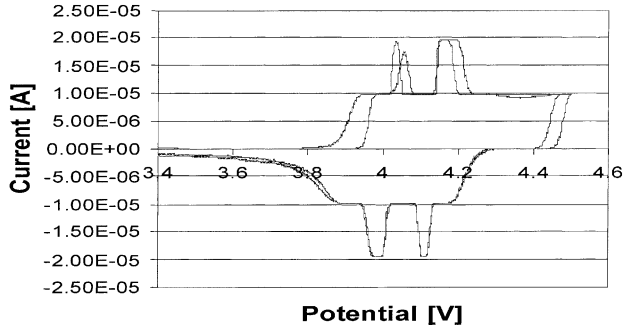

Fig. 7. Cyclic voltammogram of a LSA film cycled between 3.5 and 4.5 V vs. Li/Li^+ with 1 M $LiClO_4$ in PC electrolyte at a scan rate of 0.1 mV/s.

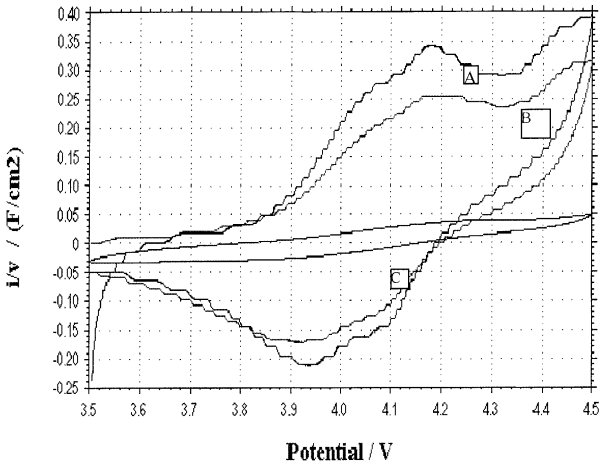

Fig. 8. Effect of scan rates on a thick $LiMn_2O_4$ film (~20 μm) grown by LSA: (A) 30 μV/s; (B) 50 μV/s; (C) 2 mV/s.

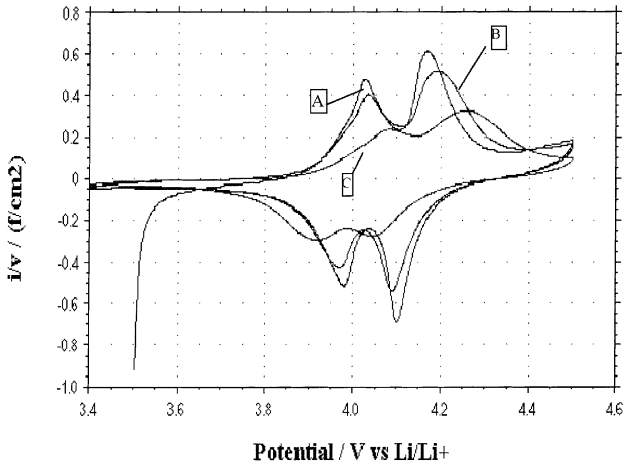

Fig. 9. Effect of scan rates on $LiMn_2O_4$ thin (0.1 μm) film: (A) 0.05 mV/s; (B) 0.1 mV/s; (C) 0.5 mV/s.

as shown in Fig. 8. The lithium intercalation and de-intercalation process is much slower for LSA deposited films. One reason for this could be the difference in the crystalline nature of the film. Lithium intercalation kinetics in a highly ordered crystalline film is much faster than that in a highly disordered or amorphous film. Kinetics did not change even when slower scan rates were used. Secondly, the mixed phase with nanocrystals in an amorphous matrix requires a higher potential to reach its equilibrium state. The highly resolved peaks seen in Fig. 9 indicate faster Li diffusion kinetics probably due to the highly crystalline nature of the films [14].

4. Conclusions

The feasibility of making $LiMn_2O_4$ thin films as the cathode material for MEMS devices by laser ablation tech-

niques was demonstrated. Thin films of $LiMn_2O_4$ were deposited on various substrate materials using two laser ablation-based techniques namely PLD and LSA. The LSA films were polycrystalline in nature with a network of nanocrystallites embedded in an amorphous matrix. Highly crystalline and textured microstructure was obtained at higher temperatures using pulsed laser deposition. These films showed good kinetics, cyclability, high charge and discharge capability with slow capacity fade. Li deficiency in the compositions was observed at higher temperatures. Laser spark atomization is a more practical approach. These films also exhibited good kinetics but lacked structural integrity.

All the above attributes make the films good candidates for their use in MEMS application. The use of higher temperature during pulsed laser deposition can be solved by the use of UV lamps. With the assistance of a UV lamp during deposition, lower substrate temperatures can be used to obtain highly crystalline as well as stoichiometric films. Results from this work will be reported in the future.

Acknowledgements

Part of this work was supported by the United States Department of Energy under the grant # DE-FG-02-98ER45722 and the Swiss Federal Office of Energy, Bern, Switzerland.

References

[1] M.M. Thackeray, W.I.F. David, P.G. Bruce, J.B. Goodenough, Mater. Res. Bull. 18 (1983) 461.
[2] David Linden, Handbook Of Batteries, Second Edition, pp. 36.1–36.14.
[3] P. Liu, J.-G. Zhang, J.A. Turner, C.E. Tracy, D.K. Benson, J. Electrochem. Soc. 146 (1999) 2001.
[4] T. Brousse, P. Fragnaud, R. Marchand, D.M. Schleich, O. Bohnke, A.K. West, J. Power Sources 68 (1997) 412.
[5] M. Morcrette, P. Barboux, J. Perriere, T. Brousse, Solid State Ionics 112 (1998) 249.
[6] D.S. Ginley, J.D. Perkins, J.M. McGraw, P.A. Parilla, Mat. Res. Soc. Symp. Proc. 496 (1998) 293.
[7] R.K. Singh, J. Narayan, Phy. Reb. B 41 (1990) 8843.
[8] D. Singh, R. Houriet, R. Vacassy, H. Hofmann, V. Craciun, R.K. Singh, in: Proceedings of the MRS Spring Meeting, 1999, in press.
[9] M.M. Thackeray, Y. Shao-Horn, A. J Kahaian, K. D Kepler, E. Skinner, J. T Vaughey, S.A. Hackney, Electrochem. Solid State Lett. 1 (1998) 7.
[10] R. Houriet, R. Vacassy, H. Hofmann, J. Mat. Res. (1999), submitted for publication.
[11] W. Yang, Q. Liu, W. Qiu, S. Lu, L. Yang, Solid State Ionics 121 (1999) 79.
[12] J.J. Xu, Andrew J. Kinser, B.B. Owens, W.H. Smyrl, Electrochem. Solid State Lett. 1 (1998) 1.
[13] Y. Park, S. Lee, B. Lee, S. Joo, Electrochem. Solid State Lett. 2 (1999) 58–59.
[14] A. Rougier, K.A. Stribel, S.J. Wen, E.J. Cairns, J. Electrochem. Soc. 145 (1998) 2975.
[15] J.B. Bates, D. Lubben, N.J. Dudney, F.X. Hart, J. Electrochem. Soc. 142 (1995) 2980.
[16] N.J. Dudney, J.B. Bates, R.A. Zuhr, S. Young, J. D Robertson, H. P Jun, S.A. Hackney, J. Electrochem. Soc. 146 (1999) 2455.